Nonlinear Beam Dynamics Experiments at the IUCF Cooler Ring

S.Y. Lee
Department of Physics, Indiana University, Bloomington, IN 47405

Abstract

Results of nonlinear beam dynamics experiments at the IUCF Cooler Ring in past two years are discussed. Our experiments include studies on (1) betatron motion at 1-D resonance island, (2) linear coupling correction, (3) Hamiltonians determined experimentally from 2-D difference and sum resonances, (4) longitudinal phase space tracking, (5) beam response to rf phase modulation, (6) beam response to rf voltage modulation, (7) synchro-betatron coupling induced by dipole field modulation and (8) attractors of a weak dissipative Hamiltonian system.

1 INTRODUCTION

There have been many nonlinear beam dynamics experiments in the past. [1-5] The beam-beam interaction Experiments at Novosibirsk VEPP-4 measured particle loss and lifetime at various nonlinear resonance conditions and similar experiments at the SPS observed large background in detector area when a high order resonance is encountered. [1] More recently, due to advances in electronics, large amounts of data can be recorded for post analysis, where the Poincaré maps becomes a powerful tool in the study of nonlinear dynamics. [3-5] Nonlinear perturbations in the accelerator include sextupoles, octupoles, and higher order multipoles. These anharmonic terms usually do not significantly perturb the particle motion in phase space except when the betatron tunes are near to a resonance condition with $m\nu_x + n\nu_z = \ell$ (m, n, ℓ integers), where the Poincaré map deviates from a simple ellipse.

This paper reports highlights of recent nonlinear beam dynamics experiments performed at the IUCF Cooler Ring, which is one of recently completed storage rings with electron cooling. [6] Fig. 1 shows the IUCF Cooler Ring geometry. The lattice properties are $C = 86.8$ m, with $\nu_x = 3.8$, $\nu_z = 4.8$ and $\hat{D}_x = 4.0$ m. The beam rigidity varies from 1 Tm to 3.6 Tm with proton kinetic energy ranges from 45 to 500 MeV. At 45 MeV, the revolution period is $T_0 = 969$ ns. The 95% emittance is electron cooled to $\epsilon \sim 0.3\pi$ mm-mrad with $\sigma_x \approx 0.7$ mm. The available dynamical aperture is about 20π mm-mrad. There are two rf systems capable of operating at harmonic numbers from $h = 1$ to 13. Our experiment started in December 1990, when the cooler experiment CE22 was approved by the Program Advisory Committee. The first test of experimental hardware was in May 1991. We completed 50 shifts of beam time in March 30, 1993 and are requesting 50 shifts for a new series of beam dynamics experiments. Currently, our hardware/software can digitize 6D phase space up to 256K turns. In past two years, we have studied $3\nu_x, 4\nu_x, \nu_x - \nu_z, \nu_x - 2\nu_z, \nu_x + 2\nu_z$ transverse resonances and studied longitudinal synchrotron Poincaré map with rf phase modulation, rf voltage modulation and the synchro-betatron coupling. From these experimental data, we were able to derive nonlinear Hamiltonian at nonlinear resonance conditions. [5-6] In section 2, the experimental procedure and some results will be reported. Section 3 will discuss future plan and conclusions.

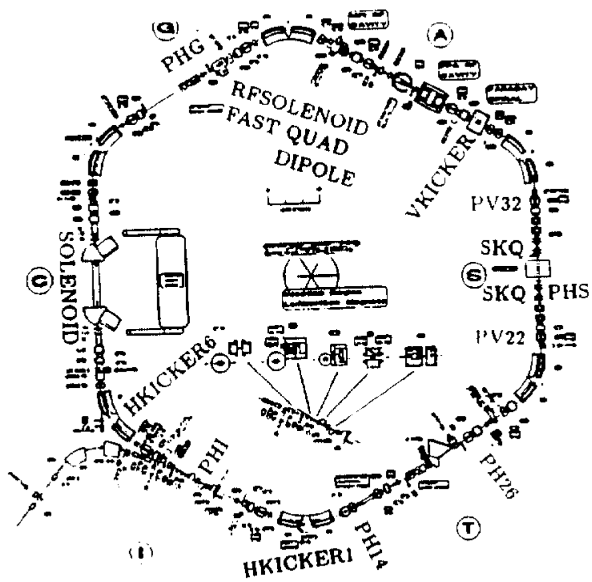

Figure 1: The schematic drawing of the IUCF Cooler Ring. The BPMs used are marked as PH or PV.

2 NONLINEAR BEAM EXPERIMENTS

Our experimental procedure started with a single bunch being kicked transversely with various transverse angular deflections, θ_K, by a pulsed deflecting magnet within one revolution or kicked longitudinally by rf phase shifter or rf phase modulation or rf voltage modulation. The subsequent beam-centroid displacement was measured by two BPMs (four BPMs for both x and z degrees of freedom) for betatron motion. The synchrotron motion was tracked by 1 BPM located at a high dispersion region with $D_x = 4.0$ m for the momentum deviation and 1 WGM or a sum signal with a phase detector relative to the rf wave to obtain the synchrotron phase. The turn-by-turn beam positions were digitized and recorded in transient recorders up to 256K memory in 8 channels for the 6D phase space. The number of turns for the particle tracking can be increased by digitizing once in every P turns (the rate divider), where P varies from 1 to 99. Important issues in these experiments are (1) the stability of beam closed orbit and be-

0-7803-1203-1/93$03.00 © 1993 IEEE

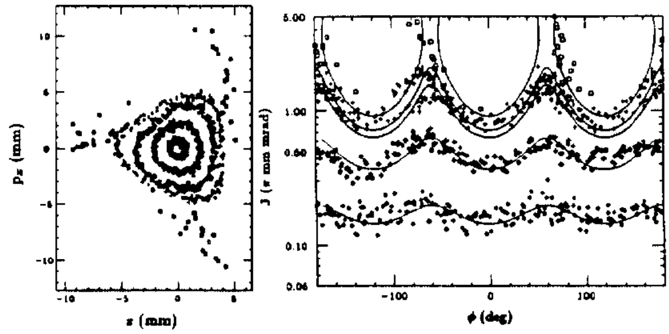

Figure 2: Poincaré maps at third order resonance.

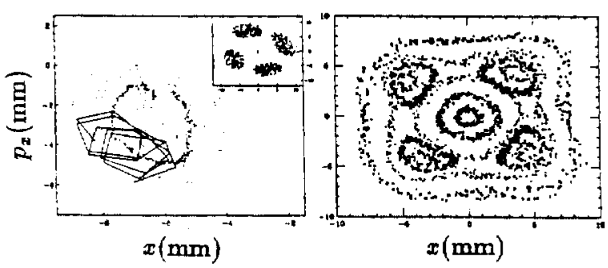

Figure 3: The Poincaré map at the fourth order resonance (left) is shown in the inset. The effect of the linear coupling motion is shown as a winding motion around an island fixed point. The Poincaré map after linear coupling correction is shown on the right.

tatron tunes, (2) the resolution of beam position monitor, (3) linearity and dynamical range of the amplifier, (4) digitization bandwidth for the time resolution and (5) careful preparation of the beam condition. Depending on physics issues, the available memory can be also important. For most of electron storage rings, the damping time is of the order of milliseconds and the betatron amplitude decoheres in hundred revolutions, the amount of memory buffer is not important. For the study of diffusion process in the hadron storage ring, large memory becomes necessary.

Besides hardware issues, beam properties in storage rings are also very important in nonlinear beam dynamics experiments. To better simulate single particle motion, nonlinear beam dynamics studies prefer a small emittance beam. The BPM measures the centroid of the charge distribution. With a smaller beam size, dynamics of resonance islands can be explored. The oscillation frequencies inside the island can be measured. The effect of betatron decoherence is smaller for smaller beam size also. When the bunch of particles is kicked to a large betatron amplitude, particles with different betatron tunes decohere in the betatron phase space. Although each particle may remain in a large betatron amplitude of a hollow beam, the centroid of the bunch becomes zero due to decoherence, which limits the number of measurable turns. Another important issue is the linear coupling, which may not destroy the island but it will mess up the interpretation of nonlinear experiments. Besides, linear coupling is also an important topic in nonlinear beam dynamics experiments, where careful measurement of $\nu_x + \nu_z = n$ resonance remains to be seen.

The conditions for most of our experiments were $h = 1$, $\eta \approx -0.86$, $\phi_0 = 0$. We chose an rf voltage of 41 V to obtain a synchrotron frequency of about 262 Hz in order to avoid harmonics of the 60 Hz ripple. Sometimes, we chose $f_{syn} = 540$ Hz in order to improve the resolution of the $\frac{\Delta p}{p}$ measurement.

2.1 Transverse Beam Dynamics Experiments

The Hamiltonian for particles encountering a single resonance, $m\nu_x + n\nu_z = \ell$, $m \geq 0$, is given by

$$H = H_0(J_x, J_z) + g J_x^{\frac{|m|}{2}} J_z^{\frac{|n|}{2}} \cos(m\phi_x + n\phi_z - \ell\theta + \chi) \quad (1)$$

where g is determined by nonlinear elements in the accelerator. The unperturbed Hamiltonian H_0, is given by $H_0(J_1, J_2) = \nu_{x0}J_x + \nu_{z0}J_z + \frac{1}{2}\alpha_{xx}J_x^2 + \alpha_{xz}J_xJ_z + \frac{1}{2}\alpha_{zz}J_z^2 + \cdots$. The Hamiltonian in the single resonance approximation is integrable. Particle trajectories follow invariant tori of the Hamiltonian flow.

A special class of the above Hamiltonian is a 1D parametric resonance, i.e. $m\nu_x = \ell$ or $n\nu_z = \ell$. Most previous experiments [2-4] was set up to study these resonances, where stable regions of phase space around stable fixed points (SFP) are called islands. The beam was kicked onto a resonance island to study properties of the Hamiltonian flow. With a small emittance beam, details of island motion could be studied. Fig. 2 shows the Poincaré maps at the third order resonance condition. The Hamiltonian for third order resonance is given by, $H = \delta J_x + \frac{1}{2}\alpha_{xx}J_x^2 + \frac{(2J_x)^{3/2}}{48\pi}F\cos(3(\phi_x + \chi))$, where ϕ_x is the betatron phase, $\delta = \nu_x - \frac{\ell}{3}$, with ℓ integer, and $Fe^{i3\chi} = \int \beta_x^{3/2}\frac{B''}{B\rho}e^{i3\phi_x}ds$ with B'' as the 2nd derivative of the magnetic field. The relative magnitude of F and $\alpha_{xx}J_x^{1/2}$ determine the characteristics of the 3rd order resonance islands. For a third order slow extraction process, a small detuning parameter and good linear coupling correction are important in achieving high efficiency.

The fourth order 1D resonance data (inset) is shown on the left side of Fig. 3. Because of the linear coupling, the Poincaré map winds around fixed points of a resonance island. The linear coupling at the IUCF Cooler may arise from the solenoidal field at the electron cooling section. Averaging the winding motion of linear coupling reveals an ellipse around an island's fixed point. [4] Eliminating the linear coupling with skew quadrupoles, the right side of Fig. 3 shows the fourth order resonance Poincaré maps [4], which give greater precision in predicting the nonlinear Hamiltonian of the synchrotron.

On the 2D ν_x–$2\nu_z = -6$ resonance, Fig. 4 shows the characteristic x, z nonlinear coupling resonance data vs revolution number. The corresponding FFT spectrum exhibits typical nonlinear coupling sidebands. Tranforming the 2D

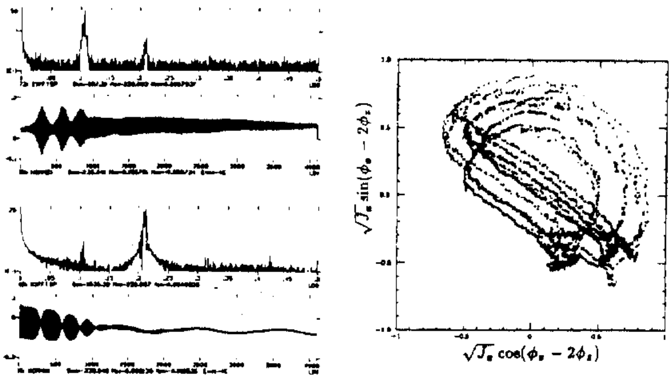

Figure 4: The measured x and z position vs turn number are shown for the experiment at $\nu_x - 2\nu_z = -6$ resonance condition. The Poincaré map in the resonance frame is shown on the right.

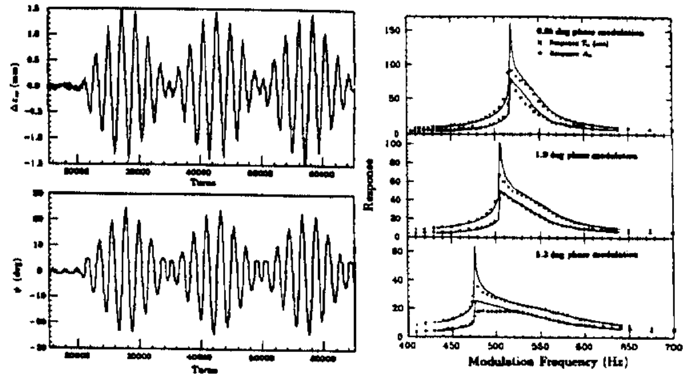

Figure 5: The response of sinusoidal modulation to the rf phase for $\frac{\Delta p}{p}$ and ϕ vs revolutions are shown on the left frame. The measured peak amplitude and the modulation period is shown as a function of the modulation frequency.

data in the resonance frame, i.e. $(\sqrt{J_x}\cos\phi_1, \sqrt{J_x}\sin\phi_1)$ with $\phi_1 = \phi_x - 2\phi_z$, the Poincaré maps in resonant frame becomes invariant tori. These data, shown in Fig. 4, was used to derive the 2D Hamitonian experimentally. [4] Although the aperture may be reduced because of the energy exchange between horizontal and vertical planes, the difference resonances are intrinsically stable. On the other hand, particle motion is unstable at a sum resonance, where the beam intensity becomes too low to make any meaningful measurement. A ferrite Panofsky quadrupole [7] was constructed to change the betatron tunes in 1 μs so that a beam bunch with reasonable intensity is tracked at the sum resonance condition. Parts of our successful initial results at $\nu_x + 2\nu_z$ resonance are reported in these proceedings. [4]

2.2 *Longitudinal Dynamics Experiments*

Longitudinal beam dynamics experiments are also important. The phase space coordinates, (ϕ, δ), with the normalized off momentum $\delta = \frac{h\eta}{\nu_s}\frac{\Delta p}{p}$, obey the mapping equations,

$$\begin{aligned} \phi_{n+1} &= \phi_n + 2\pi\nu_s\delta_n + \Delta\varphi(\theta), & (2)\\ \delta_{n+1} &= \delta_n - 2\pi\nu_s(1 + A(\theta))\sin\phi_{n+1} - \frac{4\pi\alpha}{\omega_0}\delta_n, & (3) \end{aligned}$$

where the orbital angle θ is used as the time variable, $\Delta\varphi(\theta)$ is the rf phase error, $A(\theta)$ is the rf voltage error, and α is the phase space damping coefficient due to electron cooling at the IUCF Cooler Ring. The damping time for 45 MeV protons was measured to be about 0.4 sec or $\alpha = 2.5\ \mathrm{s}^{-1}$ at an electron current of 0.75 A. Thus $\alpha \ll \omega_s$. The rf phase and voltage errors can arise from the noise of power supply or external modulation in the rf system, or from synchro-betatron coupling. The SB coupling is important to electron storage rings, where the fractional parts of the synchrotron and betatron tunes are of the same order of magnitude. For the SSC, where the synchrotron frequency varies from 7 Hz at injection energy to 4 Hz at 20 TeV, SB coupling may arise from ground vibration. At RHIC, the synchrotron frequency ramps through 60 Hz around 17 GeV/c for heavy ion beams, SB coupling may result from power supply ripple.

To understand the dynamics of synchrotron motion in the presence of phase or voltage errors, we examine first the Hamiltonian. Neglecting the damping term ($\alpha = 0$), the synchrotron equation of motion, can be derived from the Hamiltonian, $H = \frac{1}{2}\nu_s\delta^2 + \nu_s(1 + A(\theta))[1 - \cos\phi] + \delta\Delta\varphi(\theta)$. Let us transform the phase space coordinates, (ϕ, δ), into $(\tilde\phi, \tilde\delta)$ by $F_2(\phi, \tilde\delta) = (\phi - \Delta\varphi(\theta))\tilde\delta$. The new Hamiltonian becomes, $H = \frac{1}{2}\nu_s\tilde\delta^2 + \nu_s(1 + A(\theta))[1 - \cos(\tilde\phi + \Delta\varphi(\theta))]$, where the potential energy term is now independent of the momentum variable. The phase coordinate $\tilde\phi$ is relative to the revolution frequency.

Consider now the case that both the phase and the voltage errors are small and sinusoidal, i.e. $\Delta\varphi = \nu_1 a\cos\nu_1\theta$ and $A = \varepsilon\sin\nu_2\theta$ with $a, \varepsilon \ll 1$. The Hamiltonian system can be expanded in terms of the action-angle of the unperturbed Hamiltonian, i.e. $J = \frac{1}{2\pi}\oint\tilde\delta d\tilde\phi$. For our experiments with a small action, $J \le 2$, the action-angle canonical transformation can be carried out approximately by the generating function, $F_1(\phi, \psi) = -\frac{\tilde\phi^2}{2}\tan\psi$ with $\tilde\phi = \sqrt{2J}\cos\psi$, $\tilde\delta = -\sqrt{2J}\sin\psi$. The new Hamiltonian can be approximated by,

$$H \approx \nu_s J - \frac{\nu_s}{16}J^2 + \Delta H_0 + \sum_{k=1}\Delta H_{2k}^{(\pm)} + \sum_{k=0}\Delta H_{2k+1}^{(\pm)}. \quad (4)$$

The corresponding perturbed synchrotron tune is given by $\tilde\nu_s \approx \nu_s(1 - \frac{J}{8})$, which is a good approximation to the exact synchrotron tune up to about $J \approx 2.5$. The nonlinear resonance terms arising from the unperturbed Hamiltonian, $\Delta H_0 = \nu_s[-\frac{J}{2}\cos 2\psi - 2\sum_{k=1}^{\infty}(-)^k J_{2k}(\sqrt{2J})\cos 2k\psi]$, are not important because $\nu_s \le 10^{-3}$ is a small number so that the resonance condition occurs at $2k\nu_s$ = integer with a large k, where the resonance strength, proportional to J_{2k}, is very small. Here J_{2k} are Bessel functions of the first kind.

The Hamiltonian due to the external modulation induces parametric resonances at harmonics of the synchrotron frequency, i.e.

$$\Delta H_n^{(\pm)} = \begin{cases} (-)^k a\nu_s J_{2k+1}(\sqrt{2J})\sin(\nu_1\theta \pm (2k+1)\psi) \\ (-)^{k+1}\epsilon\nu_s J_{2k}(\sqrt{2J})\sin(\nu_2\theta \pm 2k\psi). \end{cases} \tag{5}$$

The resonances due to external modulation are sometimes called parametric resonances. The resonances due to the voltage modulation are located at even multiples of the synchrotron harmonics and the resonances due to the phase modulation are located at odd synchrotron harmonics. When the modulation frequency, ν_1 or ν_2, equals to the multiples of the synchrotron frequency, the coherent kick due to resonance condition dominates the beam dynamics. Making the canonical transformation to the resonance precessing frame with the generating function, $F_2(\psi, \tilde{J}) = (\psi - \frac{\nu_m}{n}\theta - \frac{\pi}{2n})\tilde{J}$, the time averaged Hamiltonian becomes,

$$\langle H\rangle = (\nu_s - \frac{\nu_m}{n})\tilde{J} - \frac{\nu_s}{16}\tilde{J}^2 - \nu_s f J_n(\sqrt{2\tilde{J}})\cos(n\tilde{\psi}), \tag{6}$$

where J_n is the Bessel function, f, aside from a possible $\pm$ sign, stands either for a or ε and ν_m stands either ν_1 or ν_2. The particle trajectory will be located on the tori of the time independent Hamiltonian flow. The longitudinal Hamiltonian is therefore almost identical to that of the transverse resonant Hamiltonian of Eq. (1). Hereafter, we drop the tilde notation for simplicity. Since the Hamitonian in Eq. (6) is time independent, it is a constant of motion. The particle trajectories, obeying the Hamilton-Jacobi equation,

$$\dot{J} = -\frac{1}{2^n n!}\nu_s c(2J)^{n/2}\sin n\psi, \tag{7}$$

$$\dot{\psi} = (\nu_s - \frac{\nu_m}{n}) - \frac{\nu_s}{8}J - \frac{\nu_s f J_n'(\sqrt{2J})}{\sqrt{2J}}\cos n\psi, \tag{8}$$

are tori with constant Hamitonian values. The fixed points, which determine charachteristics of tori, are given by $\dot{J} = 0$, $\dot{\psi} = 0$. There are in general n stable (SFP) and n unstable (UFP) fixed points. (There is a possible extra fixed point at $J = 0$ arising from the unperturbed Hamiltonian). The Hamiltonian flow corresponds to a torus about an SFP.

For illustration, we consider the lowest order parametric resonance at $\nu_m \approx \nu_s$ due to the rf phase modulation. Using $g = \sqrt{2J}\cos\psi$ with $\psi = 0$ or π as the rf phase coordinate of the fixed point, the equation for g becomes,

$$\frac{\nu_s}{16}g^3 - (\nu_s - \nu_m)g + \frac{\nu_s a}{2} = 0, \tag{9}$$

which has three possible solutions at modulation frequencies below the critical frequency ν_c called the bifurcation frequency given by $\nu_c = \nu_s[1 - \frac{3}{16}(4a)^{2/3}]$. When the modulation frequency is below ν_c, there are two SFPs and one UFP. Beyond the bifurcation frequency, only the outer SFP exists.

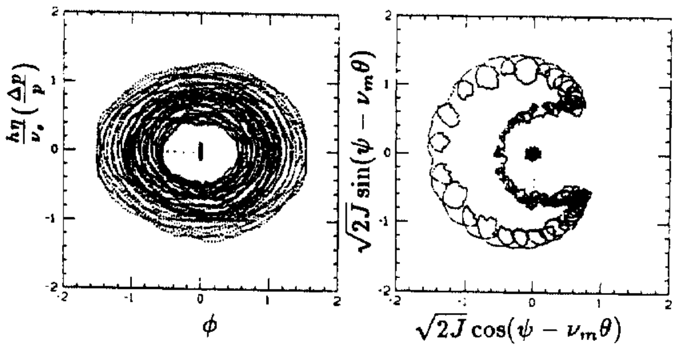

Figure 6: The response of the bunch at 42° initial phase kick to the sinusoidal modulation at a modulation amplitude of 1.3°. The Poincaré map of (δ, ϕ) is shown on the left frame and the Poincaré map in the resonance frame on the right

At the IUCF Cooler Ring, we measured Poincaré maps of the beam with phase or voltage modulations. [5] When the bunch is kicked with an rf phase shift, the synchrotron tune, measured as a function of the synchrotron amplitude, was found in excellent agreement with theory. When the rf phase is modulated sinusoidally, the response of the bunch motion located initially at the origin shows characteristics of parametric resonant system (Fig. 5). The modulation period shown in Fig. 5 characterizes the tune of the motion about an SFP. The modulation amplitude characterizes the intercept of the torus with the phase axis. The peak response and the peak modulation period occur at the same modulation frequency, which reflects the condition that the separatrix of these two resonant islands pass through the origin of the rf bucket, which is the initial condition of the beam. Figure 6 demonstrates that the reduction of the Poincaré map in the resonance frame revealing indeed the simplicity of the Hamiltonian flow of Eq. (6) from experimental data.

The rf phase modulation may also arise from synchro-betatron coupling. For proton storage rings, the synchrotron tune is small, therefore synchro-betatron coupling is usually not important. However dipole field modulation at a non-zero dispersion function location can change the circumference by $\Delta C = D_x\theta(t)$. The corresponding rf phase difference becomes, $\Delta\phi = 2\pi h\frac{\Delta C}{C}$. In our experiment, the maximum rf phase shift per turn was $\hat{\Delta\phi} = 0.78 \times 10^{-5}\hat{B}_m$ [Gauss] radians. Because the synchrotron frequency is much smaller than the revolution frequency in proton storage rings, the phase errors of each turn accumulate. The modulation phase amplitude is enhanced by the factor $\frac{\omega_0}{2\pi\omega_s}$. In this run, the injected beam was cooled and simultaneously modulated by a small dipole. A window frame ferrite dipole magnet was used to produce the transvese dipole modulation. [7] The horizontal dispersion function was $D_x \approx 4.0$ m at the modulation dipole location. The result is shown in Fig. 7, where the inset shows

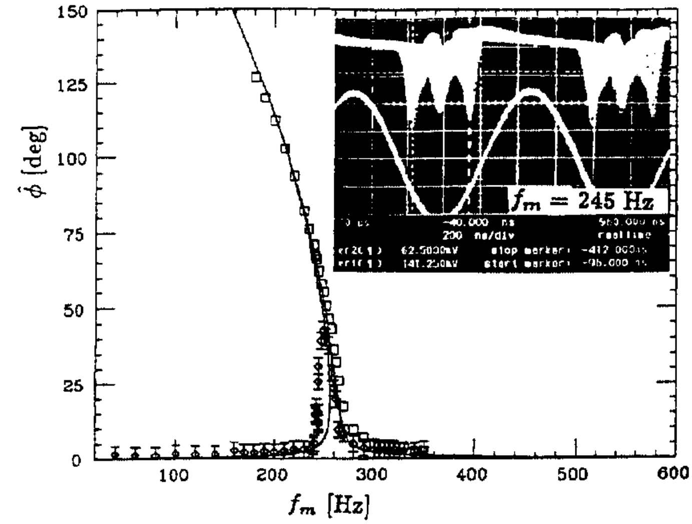

Figure 7: The inlet shows the trace of signal from a wall gap monitor triggered by the rf frequency. The measured phase amplitude of the outer beamlet is shown to compare with the fixed points of the Hamiltonian.

the trace of the bunch shape accumulated on an oscilloscope. It appears that the beam split into two beamlets. The phase amplitudes of the outer and the inner beamlets measured from the oscilloscope and digitized phase detector are also plotted in Fig. 7, where lines are solutions of Eq. (9). Because of the phase space damping due to electron cooling, particles in the phase space are trapped into the islands of the resonant Hamiltonian. These beamlets are observed to rotate about the center of the bucket at the modulation frquency. Results from similar measurements for the voltage modulation at $\nu_m \approx 2\nu_s$ indicate that the beam split into three beamlets. The measured phase amplitude of the outer beamlet agrees well with the fixed point of the Hamiltonian (6). Data analysis of these experiments will be reported shortly. [5]

3 CONCLUSION

Recent advances in fast digitizing electronics and also the availability of small emittance storage rings offer us the possibility of long term tracking of betatron and synchrotron motion. Combined with recent advances in numerical nonlinear beam dynamics methods of using the Taylor map, Lie algebraic and canonical perturbation techniques, nonlinear beam dynamics experiments are timely and important in supporting, verifying and guiding theories. Our experiments indicates that indeed a particle motion in synchrotron obeys Hamiltonian flow. In particular, the longitudinal phase space experiments reveals the simplicity of invariant tori. They are simple and predictable. Our results can therefore be used to set the tolerance for high energy accelerators on errors associated with rf voltage and phase modulations, such as ground motion, the power supply ripple etc.

The limitations of nonlinear beam dynamics experiments rest on 1) finite beam size, 2) decoherence of betatron motion, 3) uncontroled tune modulation. These limitations reflect however a realistic storage ring environment. Theoretical calculations are usually limited by its difficulties in predicting the realistic environment. Our next phase of experiments will begin with rf phase/voltage modulation to create longitudinal island structure and study the particle motion when a second harmonic modulation at the island tune is applied. However, transverse beam dynamics remains to be our major focus. With a successful sum resonance experiment [4] by using the Panofsky quadrupole for the tune jump, we will study 2-D resonances. We will not forget the survival plot either. All these experiments require careful planning and beam conditioning. These difficult experiments have just begun to take place.

Acknowledgement

Work supported in part by a grant from NSF PHY-9221402. I benefit greatly from discussions with members of the CE22 collaboration.

4 REFERENCES

[1] A.B. Temnykh, p.5, Proc. of the 3rd Adv. ICFA beam dynamics workshop, ed. I. Koop and G. Tumaikin, Novosibirsk (1989); L. Evans, et.al., Proc. of EPAC Rome, p.619, (1988); L. Evans, J. Gareyte, A. Hilaire, and F. Schmidt, Proc. of IEEE PAC, Chicago, p. 1376 (1989); L. Evans, et.al., ibid. 1403(1989); L. Evans, CERN SPS/83-38;

[2] M. Cornacchia and L. Evans, Part. Accel. 19, 125(1986); P.L. Morton, et. al., IEEE Tran. Nucl. Sci. NS-32, 2291 (1985). D.A. Edwards, R.P. Johnson, and F. Willeke, Part. Accel. 19, 145 (1986). A. Chao, et al., Phys. Rev. Lett. 61, 2752 (1988); N. Merminga, et al., Proc. EPAC, p.791 (1988). T. Satogata, et al., Phys. Rev. Lett., 68, 1838 (1992); P. Krejcik, Proc. ICFA Beam Dynamics Workshop II (Lugano), CERN 88-04, p.145 (1988).

[3] J. Bridge, et al., Part. Acc. 28, 1 (1990). E. Crosbie, et al., IEEE PAC, p.1624 (1991); J. Liu, et al., Ph.D. Thesis, Univ. of Wisconsin, (1993) unpublished.

[4] S.Y. Lee, et al., Phys. Rev. Lett. 67, 2767 (1991); D.D Caussyn, et al., Phys. Rev. **A46**, 7942 (1992); M. Ellison, et al., these proceedings, Y. Wang, et al., these proceedings.

[5] M. Ellison, et al., Phys. Rev. Lett. **70**, 591 (1993); D.D. Caussyn et al., these proceedings; M. Syphers, et al., "Experimental Study of Synchrotron Coupling and Strange Attractors", submitted to the Phys. Rev. Lett., March (1993); these proceedings. Y. Wang, et al., "On Synchro-Betatron Coupling induced by Dipole Modulations", to be published; H. Huang, et al., "Experimental determination of the Hamiltonian for synchrotron motion with the rf phase modulation", to be published; D. Li, et al., "Experimental measurement of resonance islands induced by the rf voltage modulation", to be published.

[6] R.E. Pollock, Proc. of IEEE Part. Acc. Conf., p.17 (1989).

[7] J. Budnick, T. Hall, D. Li, S.Y. Lee, these proceedings.